Environmental and Climate Technologies
2025, vol. 29, no. 1, pp. 285–299
https://doi.org/10.2478/rtuect-2025-0020
https://content.sciendo.com

Urban Sewage Treatment Monitoring Based on 3DEEM Regional PCA

Zonghua WANG[1], Xiaohang MA[2*], Jun ZHANG[3], Li DU[4]

[1–3]*School of South to North Water Diversion/School of Water Resources and Modern Agriculture, Nanyang Normal University, Nanyang 473061, China*

[4]*College of Life Science and Agricultural Engineering, Nanyang Normal University, Nanyang 473061, China*

Received 10.09.2024; accepted 08.05.2025

Abstract **– Urban sewage treatment, as a key task of modern environmental engineering, plays a crucial role in ensuring public health, environmental protection, and sustainable utilization of water resources. However, as the concentration and types of organic pollutants in wastewater increase, the monitoring task of wastewater treatment has become a major challenge. The study used the three-dimensional excitation emission matrix fluorescence spectroscopy regional principal component analysis method to analyze and track the conversion and removal efficiency of organic matter in the wastewater treatment process in detail. Research has found that the regional similarity of aromatic protein substances decreased from 90.06 % to 88.26 %. The regional similarity of microbial metabolites decreased from 89.53 % to 87.91 %, indicating a relatively stable transformation of microbial metabolites. The regional values of humic acid and humic acid substances decreased from 77.88 % and 77.61 % to 71.01 % and 66.11 %, respectively. The study validated the application value of the given regional principal component analysis method in monitoring organic matter changes in urban sewage treatment processes, providing quantitative basis for understanding the behavior patterns of different organic substances in sewage treatment processes. This method provides scientific guidance for optimizing treatment processes and improving water quality. It promotes the development of urban sewage treatment technology and the progress of environmental protection work.**

Keywords **– Three-dimensional excitation emission matrix fluorescence spectroscopy; regional integration method; principal component analysis method; urban sewage treatment; water quality indicators.**

1. INTRODUCTION

Urban sewage treatment, as a key link in maintaining water resource recycling and ecological balance, always show significant position in the fields of environmental engineering and public health [1]. Under industrialization and urbanization, the quantity and complexity of urban sewage have significantly increased [2]. Traditional water quality monitoring methods are no longer able to satisfy the needs of quickly and accurately evaluating the effectiveness of sewage treatment. Exploring efficient real-time monitoring technologies is of great significance for improving the management level of urban sewage treatment and ensuring water quality safety [3]. Three-dimensional excitation emission

* Corresponding author.
E-mail address: XiaohangMa2013@outlook.com

matrix fluorescence spectroscopy (3DEEM) technology is widely used in the analysis of organic matter in complex water bodies due to its high sensitivity and rapid response [4]. The combination of region integration method can effectively analyze fluorescence spectral data, providing a new approach for the characterization of complex organic compounds in wastewater [5]. Meanwhile, the introduction of Principal Component Analysis (PCA) further enhances the multidimensional and analytical capabilities of data processing, providing a powerful tool for decoding subtle changes in wastewater treatment processes. Based on this background, the study adopts 3DEEM combined with regional integration method and PCA to apply to urban sewage treatment monitoring, aiming to achieve efficient tracking and evaluation of the entire sewage treatment process. It is hoped to achieve real-time monitoring of water quality changes during urban sewage treatment through this method, in order to ensure that the effluent quality meets the standards and provide scientific decision-making basis for sewage treatment. The innovation of the research lies in combining 3DEEM technology with advanced data processing methods, providing a new approach and tool for real-time monitoring of urban sewage treatment, in order to promote the development of environmental monitoring technology to a higher level.

There are mainly five parts. The first elaborates on the limitations of urban sewage treatment in environmental protection, water resource management, and current water quality monitoring technologies in terms of treatment efficiency and accuracy. The second elaborates on the research progress of 3DEEM technology in water quality monitoring. The third part is the application of 3DEEM technology in urban sewage treatment monitoring. The first section provides an overview of the basic principles of 3DEEM and its ability to analyze organic matter composition in wastewater. The second section explores the optimization of 3DEEM data processing and application using regional integration analysis methods. The fourth part tests the algorithm proposed in this study. The fifth part is a summary and outlook of this study.

2. RELATED WORK

Since the birth of 3DEEM technology, its application in environmental monitoring and water quality analysis has gradually become a research hotspot, and many scholars have conducted research on 3DEEM technology. Venturini *et al*. proposed a quality evaluation method for olive oil that integrates neural network with fluorescence spectroscopy. It can quickly determine five olive oil indicators through a fluorescence. The research results indicated that this method accurately predicted ethyl ester content, achieving timely and cost-effective quality control in the production cycle [6]. Lee *et al*. proposed that coherent vibrational spectra recorded using time-resolved fluorescence technology could reveal the vibrational characteristics of emitted molecules and served as a tool for studying excited state molecular dynamics. The research results indicated that through the analysis of Schiff base salicylaldehyde, it has been determined that intramolecular proton transfer occurred within 22 femtoseconds and was limited to one side of the molecule [7]. Xu *et al*. proposed a fast fluorescence recognition network model for analyzing fluorescence signals. The research results indicated that by processing a single 3DEEM using convolutional neural networks, the model could accurately classify the number of fluorescent components with a high accuracy of 0.956 and predicted their distribution with a low average absolute error of 8.9×10^{-4}. The accuracy improved with the increase of training data [8]. Tang *et al*. proposed a three-dimensional guaranteed conservative transport model supported by the finite volume, which was implemented on a cubic spherical mesh. The research results indicated that the model could use a large Courant number on any dense vertical grid, and further improve the accuracy of numerical solutions through singular splitting techniques and nonnegative corrections, demonstrating its potential in practical atmospheric simulation applications [9]. Cheng *et al.* used the crude oil characteristics to distinguish the types and sources of crude oil in multi-source oil and gas systems. The research results indicated that an increase in thermal maturity led to a slight increase in the average fluorescence lifetime value of pyrolysis oil, while at a specific maturity λ-τ, the mode remained unchanged. The TRES fluorescence lifetime parameter not only effectively classified different crude oils but also combined physical and geochemical parameters to identify the thermal maturity from the same source. It had significant potential for identifying petroleum inclusions from multi-source oil and gas systems [10].

With the increasing demand for urban sewage treatment, the combination of 3DEEM technology and PCA method has shown great potential in treating complex water sample data, and many scholars have conducted considerable research on PCA method. Han L. *et al.* proposed the use of in-situ carbothermal reduction/partial sintering technology to synthesize six element high entropy transition metal carbide aerogels. The results showed that the synthesized aerogel had a uniform microstructure at 1773 °C, the particle phase and pore size were 100–300 nm and 0.2–10 μm, and the density was 0.45 g/cm³. It had a high porosity of 94.5 % and a compressive strength of 0.8 MPa [11]. Xue *et al.* used high-speed countercurrent chromatography to isolate dihydromyricetin with a purity of 97.13 % from grape plants. The research results indicated that the interaction between dihydromyricetin and corn starch affected its structure and function through hydrogen bonding and non covalent bonding, improved the relative crystallinity of corn starch, reduced spin relaxation time, and slowed down the migration of free water [12]. Kassinopoulos *et al.* proposed a framework for evaluating the performance of functional magnetic resonance imaging data preprocessing pipelines, which quantified the reduction of signal-to-noise ratio and motion artifacts through a simplified set of quality control indicators. The research results indicated that the quality control index scores were highest when removing global signals and white matter principal components. In addition, the application of mild white matter denoising can further improve data quality without the need for scrubbing techniques [13]. Ameek *et al.* proposed a PCA method for the flux of polycyclic aromatic hydrocarbons in NGC 7023 nebula. The research results indicated that two principal components could explain 98 % of the observed variation in polycyclic aromatic hydrocarbon flux, with the first principal component representing total PAH emissions and the second principal component correlated with the ionization state of polycyclic aromatic hydrocarbons. The correlation analysis revealed the existence of two ion band subgroups, and the independent PCA inside the cavity suggested that the second principal component may be related to the structural changes of polycyclic aromatic hydrocarbons rather than the charge state [14]. Moreno *et al.* proposed a statistical classification method based on the characteristics of foaming agents, which was based on molecular weight, hydrophile lipophilic balance. The research results indicated that PCA transformed these seven features into three main components, explaining 64.4 % and 27.7 % of the variance, respectively [15].

In summary, 3DEEM technology, due to its high sensitivity and rapid response ability to organic matter in complex water bodies, provides an efficient technique for environmental monitoring. However, in practical applications, optimizing data processing flow, improving model generalization ability, and reducing the complexity of instrument operations remain major challenges. Therefore, the study adopts 3DEEM regional PCA for monitoring urban sewage treatment, aiming to enhance environmental protection.

3. URBAN SEWAGE TREATMENT MONITORING TECHNOLOGY BASED ON 3DEEM

The study delved into the application of 3DEEM technology in urban sewage treatment monitoring. The regional integration analysis method is used to deconstruct 3DEEM data to identify and quantify key chemical components in wastewater. In addition, the application of PCA aims to reveal the interactions and changing trends of various components in the wastewater treatment process. The combination of these methods will help improve the accuracy and efficiency of sewage treatment monitoring. It is hoped to provide new basis for urban sewage treatment and open new perspectives for environmental monitoring and management.

3.1. Regional Integration Analysis Method Based on 3DEEM Data

In order to more accurately monitor and evaluate the effectiveness of urban sewage treatment, and to quantitatively reveal the fluorescence characteristics of each component in water quality, the key information about water quality indicators is needed [16]. The research studies a regional integration analysis method based on 3DEEM technology and performs regional integration processing on 3DEEM data. The principle of its three-dimensional fluorescence generation is shown in Fig. 1.

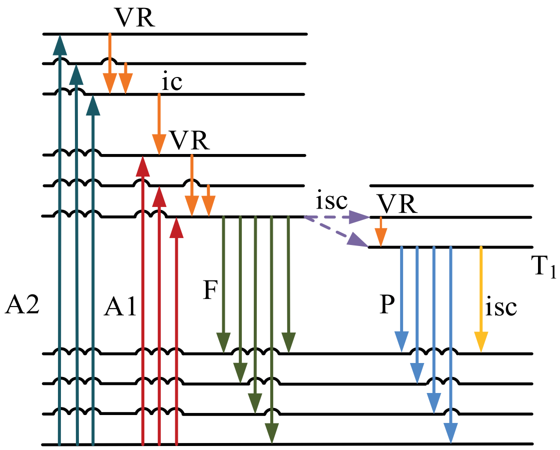

Fig. 1. The principle of generating three-dimensional fluorescence spectra.

3DEEM technology displays the fluorescence characteristics of the sample through a two-dimensional matrix of excitation and emission wavelengths, thereby analyzing the composition information of sewage components [17]. Through simplifying 3DEEM data into representative feature parameters, the integral regions are identified [18]. When the incident light comes into contact with the surface of a substance, some fluorescent genes in the substance molecules will absorb some of the photon energy of the incident light. The mathematical expression for the light absorption process is shown in Eq. (1).

$$E_1 - E_0 = hv = hc / \lambda , \tag{1}$$

where
E_1 the initial energy of the incident light;
E_0 the remaining energy of the incident light;
h the Planck constant;
v the light frequency;
c the speed of light;
λ the wavelength of light

In Eq. (1), the fluorescence quantum yield represents the ratio of the number of light quanta emitted and absorbed by a substance during the process of generating fluorescence, and its definition formula is given as Eq. (2).

$$\phi = \frac{N_e}{N_a} , \tag{2}$$

where
N_e the number of photons emitted by the substance;
N_a photons absorbed by a substance.

The fluorescence quantum yield ϕ can be explained by the rate constants of energy release at different stages, and its mathematical definition is shown in Eq. (3).

$$\phi = \frac{K_f}{K_f + \sum K_i} , \tag{3}$$

where
K_f symbol that shows the constant of fluorescence generation rate;
$\sum K_i$ represents the sum of the rates of all non-radiative transitions, such as inter system transitions, and is generally influenced by the chemical environment surrounding the fluorescence generation process

The 3DEEM data generated by sewage bodies are shown in Table 1.

TABLE 1. 3DEEM DATA GENERATED BY SEWAGE WATER BODIES

Fluorescence peak	Water inlet	Delivery port	Anoxic pool	Anaerobic tank	Aerobic tank
Fluorescence peak T1	6835	4489	3577	2763	2494
Fluorescence peak T2	5596	3798	3318	2571	2367
Fluorescence peak FA	2283	2057	1998	2003	2059
Fluorescence peak HA	2091	2014	2035	2016	1907

During the sewage treatment process, there are significant differences in the degradation of organic matter in the water at different stages from the inlet, anoxic tank, anaerobic tank, aerobic tank to the outlet. The regional integration analysis method quantitatively processes such data and analyzes the changes in fluorescence characteristics at each processing stage. Among them, temperature determines the fluorescence intensity and fluorescence efficiency, and the definition formula for the relationship between the two is shown in Eq. (4).

$$(F_0 - F)/F = ke^{-E/RT}, \tag{4}$$

where

F_0 represents the fluorescence intensity in the initial state;
F represents the fluorescence intensity after a temperature rise;
E represents the additional energy required for the molecule;
T symbol that shows thermodynamic temperature;
R the symbol of the gas constant.

Through regional integration analysis, the research accurately evaluates the removal efficiency of each treatment unit and its mechanism of action on specific organic pollutants. The region integration method is used for 3DEEM data, and its region division is shown in Fig. 2.

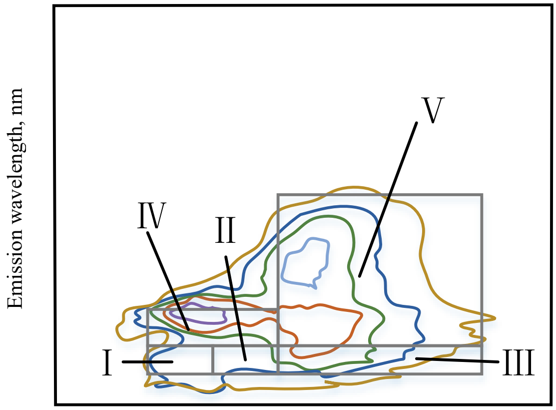

Fig. 2. Region division based on 3DEEM data using region integration method.

The application of 3DEEM technology in wastewater treatment analysis can finely identify and quantify organic substances in water samples through regional integration method. Under regional integration analysis, fluorescence spectral data is divided into specific regions, each corresponding to a different category of organic matter. The region integration analysis of 3DEEM data divides the fluorescence region into five parts. The formula for integrated volume of the fluorescence region is given as Eq. (5).

$$\begin{cases} \Phi_{i,n} = MF_i \Phi_i \\ \Phi_i = \int_{ex}\int_{em} I(\lambda_{ex}\lambda_{em}) \mathrm{d}\lambda_{ex}\lambda_{em} \end{cases}, \tag{5}$$

where

$\Phi_{i,n}$ the standardized integrated volume of the region I;

Φ_i the integrated volume;

MF_i the multiplication factor;

$I(\lambda_{ex}\lambda_{em})$ the fluorescence intensity.

The calculation formula for the total fluorescence area volume is shown in Eq. (6).

$$\begin{cases} \Phi_{T,n} = \sum_{i=1}^{5} \Phi_{i,n} \\ P_{i,n} = \Phi_{i,n} / \Phi_{T,n} \times 100\,\% \end{cases}, \tag{6}$$

where $\Phi_{T,n}$ is standardized integrated volume of the total fluorescence region, and $P_{i,n}$ is the ratio of regional standardized integrated volume to the total standardized integrated volume.

By integrating these regions, the concentration changes of various organic pollutants in wastewater can be quantitatively analyzed, and the organic matter removal efficiency during wastewater treatment can be monitored.

3.2. The Application of PCA in Wastewater Treatment Monitoring

In urban sewage treatment monitoring, PCA combined with regional integration method can clarify the changing trends of various main components at different treatment stages [19]. By combining 3DEEM and PCA methods, key information can be extracted from complex 3DEEM data, simplifying the data processing process and achieving analysis of the main pollutant characteristics in urban sewage treatment. The main process flow of sewage treatment is shown in Fig. 3.

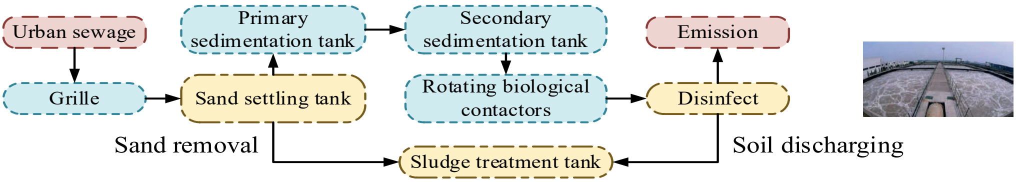

Fig. 3. Main process flow of sewage treatment.

The sewage treatment process involves multiple steps, each of which has an impact on water quality indicators [20]. In this process, PCA monitors and evaluates the effectiveness of each processing stage. Analyzing the most important pollution characteristics in wastewater provides data support for understanding and optimizing the treatment effectiveness of each key link. Assuming that there are m indicator variables for PCA, including n evaluation objects, the value of the indicator j of the evaluation object i is x_{ij}, and the values of each indicator are converted into standardized indicator $\tilde{x}_{ij}$. The expression is shown in Eq. (7).

$$\tilde{x}_{ij} = \frac{x_{ij} - \tilde{x}_j}{s_j}, (i = 1, 2, \ldots, n; j = 1, 2, \ldots, m) \tag{7}$$

where

s_j the sample mean and sample standard deviation of the j-th indicator;

$\tilde{x}_j$ a standardized indicator variable. Established correlation coefficient matrix R between variables, and its mathematical expression is shown in Eq. (8).

In Eq. (8), r_{ij} represents the correlation coefficient between the i-th and j-th indicators.

$$\begin{cases} R=(r_{ij})_{(m\times m)} \\ r_{ij}=\dfrac{\sum_{k-1}^{m}\tilde{x}_{ij}\cdot\tilde{x}_{kj}}{n-1},(i,j=1,2,\ldots,m) \end{cases} \tag{8}$$

This provides a scientific basis for developing more precise treatment strategies and improving the overall performance of sewage treatment systems. The regional principal component division of 3DEEM is shown in Fig. 4.

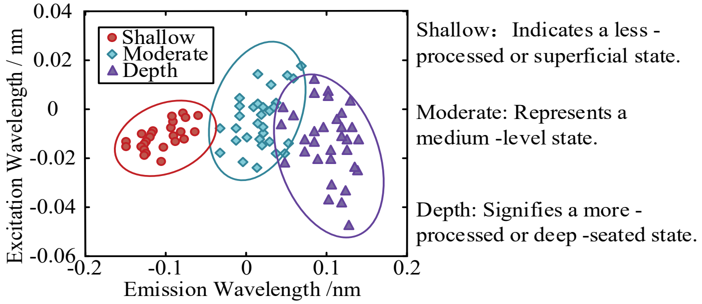

Fig. 4. Regional Principal Component Division of 3DEEM.

In the field of sewage treatment monitoring, 3DEEM region combined with PCA to accurately classify the regional principal components of organic matter. Each divided area represents different groups of organic matter, such as proteins and humic substances. The mathematical expression for extracting principal components and calculating comprehensive scores is shown in Eq. (9).

$$Z=\sum_{j=1}^{p}b_j y_j \tag{9}$$

where y_i is the i-th principal component, p represents the indicator variable, and b_j is the symbol that shows the information contribution rate.

When simplifying the dataset using PCA, maintain maximum interpretability of the original information to clarify the pollutant removal efficiency of various processing stages such as anaerobic, anaerobic, and aerobic tanks. The characteristic peak fluorescence intensity of urban sewage components based on 3DEEM regional PCA is shown in Fig. 5.

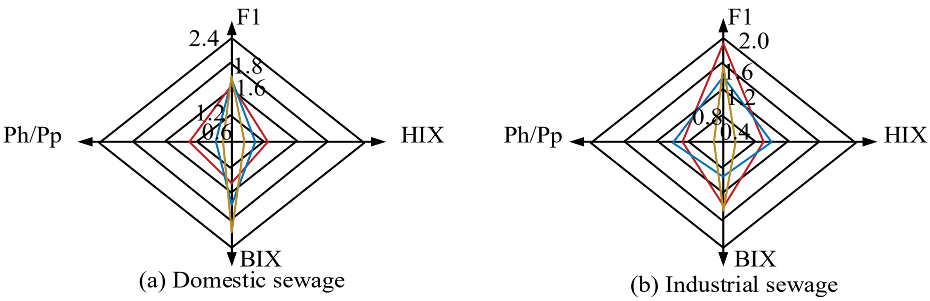

Fig. 5. A Fluorescence intensity of characteristic peaks of urban sewage components based on 3DEEM regional PCA.

The construction of radar images is based on peak fluorescence intensity, which can intuitively reflect the characterization characteristics of different pollutants in fluorescence spectra [21]. By using radar images, significant organic components such as humic acid, fulvic acid, and protein substances can be clearly identified in sewage samples. Using the PCA method of MATLAB to perform component analysis on three-dimensional fluorescence matrix data E_{ij}, then its covariance matrix is obtained, as Eq. (10).

$$c_{ij} = \mathrm{cov}(X_i Y_j) = E\left\{[X_i - E(E_i)][X_j - E(E_j)]\right\}, \tag{10}$$

where i is the symbol that shows the excitation wavelength selection point, j represents the emission wavelength selection point. The formula for calculating the principal component score in the sample is shown in Eq. (11).

$$\begin{cases} (A_z)_{jk} = \sum_{j=1}^{p} w_j \cdot z_k \\ z_k = \dfrac{c_k - \bar{c}}{\sigma} \end{cases}, \tag{11}$$

where

z_k represents the standardized concentration of sewage pollutants at the k observation point;

$(A_Z)_{jk}$ represents the score value;

W_j the symbol that shows the factor coefficient;

c_k the symbol that shows the concentration of sewage pollutants at point k;

$\bar{c}$ represents the arithmetic mean of the concentration of pollutants in wastewater;

σ represents the standard deviation of pollutant concentration in wastewater.

This analysis method not only enhances the understanding of the complexity of sewage composition but also provides strong data support for monitoring sewage treatment efficiency and optimizing related processes.

4. Experimental Analysis of Sewage Treatment Monitoring Based on 3DEEM and PCA

This chapter detailed the monitoring of wastewater treatment processes using 3DEEM combined with PCA method. Firstly, fluorescence data of different water quality samples were collected through 3DEEM, and the effects of various water quality indicators such as chemical oxygen demand (COD), ammonia nitrogen (NH_3-N), and total phosphorus (TP) on 3DEEM spectra were evaluated. Secondly, the correlation between 3DEEM parameters and the aforementioned water quality indicators was explored. By conducting PCA dimensionality reduction analysis, the research aimed to reveal the characteristic information of various components in wastewater and the effectiveness of wastewater treatment, providing a reliable monitoring method for optimizing the wastewater treatment process.

4.1. Evaluation Experiment of 3DEEM Response to Different Water Quality Indicators

For getting the accuracy and reliability of this study, testing and analysis were conducted in a controlled experimental environment. The laboratory temperature and humidity were maintained at 23±1 °C and 50±5 %, respectively. After collecting sewage samples, the

HORIBA Aqualog-800 model 3DEEM instrument with high sensitivity and resolution should be used for sample testing. To obtain accurate fluorescence data, the excitation wavelength range of the instrument was set to 200–800 nm, the emission wavelength range was 250–830 nm, and the wavelength interval between excitation and emission was set to 5 nm. The data collection and processing were carried out using Aqualog software to ensure the accurate drawing and analysis of fluorescence spectra. In terms of hardware environment, the experiment used a computer equipped with Intel Core i7 processor and 16 GB RAM for high-speed data processing and complex computing. 3DEEM combined with PCA method could comprehensively reflect the fluorescence characteristics of organic substances in water, and through dimensionality reduction processing, reveal the characteristics and structural information behind the data. By accurately capturing the fluorescence response of organic components in wastewater, this experimental analysis provided scientific indicators for the comprehensive evaluation of sewage treatment effectiveness. The changing trends of different water quality indicators are shown in Fig. 6.

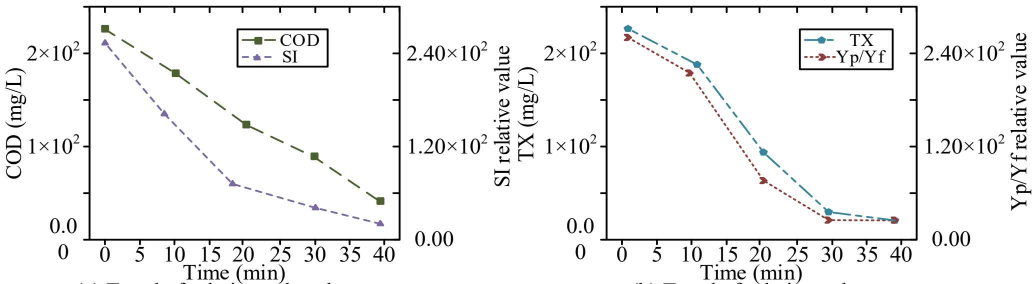

(a) Trend of relative value changes between COD and SI

(b) Trend of relative value changes between TX and Yp/Yf

Note:
COD: Chemical Oxygen Demand, a measure of the oxygen required to chemically oxidize organic and certain inorganic substances in water, expressed in mg/L;
SI: Likely a specific water - quality - related index (e.g., a synthetic or study - defined index), presented as a relative value;
TX: Potentially a total or composite indicator (e.g., total fluorescence - related or treatment - specific index), shown as a relative value in mg/L (note: units might need adjustment based on study context);
Yp/Yf: A ratio of two parameters (e.g., peak - to - fundamental fluorescence intensities or other study - defined variables), presented as a relative value.

Fig. 6. The changing trends of different water quality indicators.

In Fig. 6(a), the COD value shows a decreasing trend with time, with an initial value of 2.34×10^2. After a certain period of time, it eventually dropped to 0.79×10^2. SI also showed a decreasing trend over time, decreasing from 2.18×10^2 to 0.49×10^2. It indicated that with the extension of treatment time, organic pollutants were significantly degraded, reflecting the improvement of treatment efficiency. In Fig. 6(b), both TX and Yp/Yf exhibit a clear decreasing trend over time. The relative value of TX declined from approximately 2.36×10^2 to 0.64×10^2, while Yp/Yf decreased from about 2.20×10^2 to 0.63×10^2. This parallel reduction indicates that not only the total organic load but also the protein-like and humic-like components were effectively removed. The consistent downward trend of these indicators demonstrates the system's strong and sustained capability in degrading complex organic substances during the treatment process.

TABLE 2. FLUORESCENCE PRINCIPAL COMPONENT FRACTION OF WATER QUALITY INDICATORS UNDER DIFFERENT PROCESSES

Similarity	**Water inlet, %**	**Anaerobic tank, %**	**Anoxic pool, %**	**Aerobic tank, %**	**Delivery port, %**
First principal component	86.51	91.02	90.07	95.68	96.13
Second principal component	3.75	3.03	3.39	3.99	3.05
Third principal component	2.36	2.43	2.41	0.72	1.84
Fourth principal component	2.18	1.16	2.15	0.97	1.62

As shown in Table 2, during the water treatment process, the proportion of the first principal component steadily increased from 86.51 % at the inlet to 96.13 % at the outlet, indicating that the proportion of the first principal component in the water quality index was increasing, and it achieved centralized purification or showed higher stability in subsequent treatment processes. The second principal component showed little variation in each processing stage, with overall slight fluctuations ranging from 3.75 % to 3.99 %. The third principal component significantly decreased to 0.72 % in the aerobic pool, far lower than the values of 2.36 % to 2.43 % in other stages. The changes of the fourth principal component in each stage were also different, but the overall proportion was relatively small, decreasing from 2.18 % at the inlet to 1.62 % at the outlet, indicating that its related indicators were gradually degraded or transformed during the water treatment process. The initial characteristic values and pollution contribution rates of different water quality indicators are shown in Fig. 7.

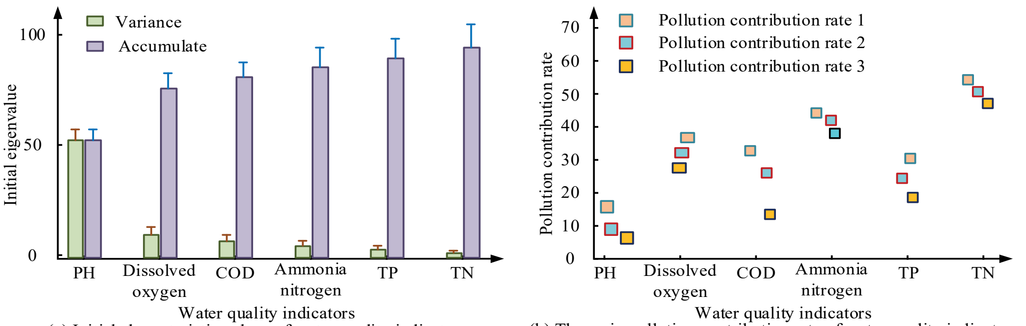

(a) Initial characteristic values of water quality indicators (b) The main pollution contribution rate of water quality indicators

Fig. 7. Initial characteristic values and pollution contribution rates of different water quality indicators.

In Fig. 7(a), the variance of the water quality parameter pH value was 54.16, and its cumulative variance contribution rate showed consistency, verifying that the proportion of pH in total variation was relatively significant. The variance of COD was 6.57, and the cumulative variance contribution rate reached 91.17. The variance of TP was 1.06, and the contribution rate was 99.11, indicating that although TP had a small contribution to the total variation of water quality, its cumulative impact was significant. This revealed its relatively small contribution in cumulative variance, but it almost occupied a complete contribution in overall water quality variation. In Fig. 7(b), the average pollution contribution rate of pH was 7.96 %, indicating the stability of its impact on overall pollution. The average pollution contribution rate of COD was 31.38 %. The average pollution contribution rate of dissolved oxygen was 4.05 %. The average pollution contribution rate of TP was 19.86 %. The average pollution contribution rate of total nitrogen was 17.59 %. The precise calculation and comparison of these data provide key indicators for water quality management, which is crucial for developing targeted pollution control strategies.

4.2. Experimental Analysis of the Correlation between 3DEEM Monitoring and Water Quality Indicators

The 3DEEM method and PCA can accurately monitor and analyze organic substances in wastewater, providing an effective scientific basis for processing large amounts of spectral data. Exploring the correlation between 3DEEM monitoring data and traditional water quality indicators can optimize monitoring strategies and achieve real-time tracking of water quality changes. The correlation analysis between the regional integration values of various substances in the spectrum and chemical COD and total nitrogen is shown in Fig. 8.

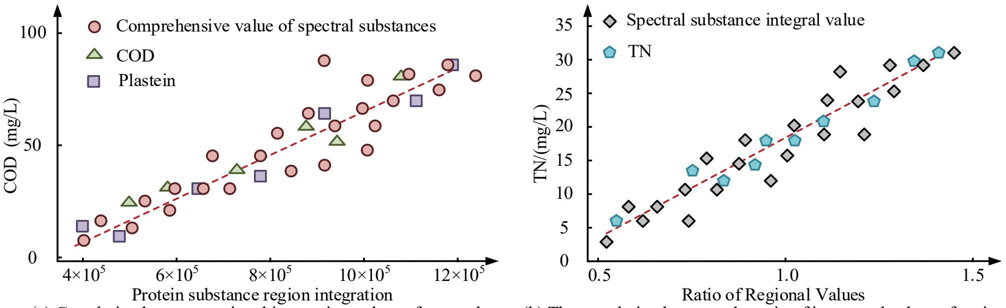

(a) Correlation between regional integration values of spectral substances and chemical oxygen demand

(b) The correlation between the ratio of integrated values of various substances in the spectrum and total nitrogen

Fig. 8. Correlation analysis between regional integration values of spectral substances and chemical oxygen demand and total nitrogen.

In Fig. 8(a), the average regional integration value of COD reached 8.16×10^5, reflecting the total amount of COD in the studied area. The average integration value of protein regions was 8.62×10^5. In Fig. 8(b), the ratio of regional values of total nitrogen was quantitatively 1.08, showing the comparative relationship of total nitrogen content between different sampling areas. The regional value ratio of total nitrogen ranged from 0.67 to 1.25, reflecting the relative differences of total nitrogen in different sampling areas. The correlation analysis between different water quality indicators is shown in Fig. 9.

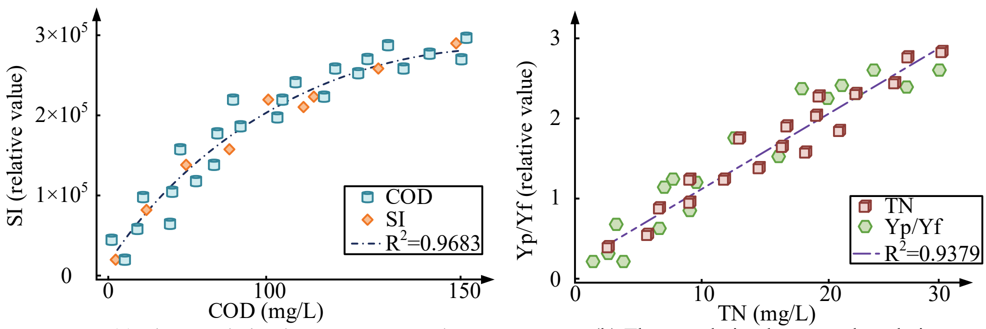

(a) The correlation between COD and SI relative values

(b) The correlation between the relative values of TN and Yp/Yf

Fig. 9. Correlation analysis between different water quality indicators.

In Fig. 9(a), the increase in COD concentration was directly proportional to the correlation with SI. When the COD concentration was 21.37 mg/L, the relative value of SI was recorded as 0.21×10^5. As the COD concentration increased to 119.89 mg/L, the relative value of SI significantly increased to 2.13×10^5. When the COD concentration reached 218.79 mg/L, the relative value of SI further increased to 2.75×10^5. At different concentrations of COD, the increase in pollutant saturation showed a certain dependence, which was related to the cumulative effect of pollutants in the water. In Fig. 9(b), as the TN concentration increased, the Yp/Yf ratio also showed an increasing trend, where Yp represented production potential and Yf represented actual production value. When the TN concentration was 3.59 mg/L, the Yp/Yf ratio was 0.46. As the TN concentration increased to 10 mg/L, the ratio significantly increased to 1.42. When the TN concentration further increased to 30 mg/L, the Yp/Yf ratio increased to 2.86. The similarity results between the integrated values of each region and the three-dimensional fluorescence peaks of each region are shown in Table 3.

TABLE 3. THE SIMILARITY RESULTS BETWEEN THE INTEGRATED VALUES OF EACH REGION AND THE THREE-DIMENSIONAL FLUORESCENCE PEAKS OF EACH REGION

Similarity	**Water inlet, %**	**Anaerobic tank, %**	**Anoxic pool, %**	**Aerobic tank, %**	**Delivery port, %**
Regional value of aromatic protein substances	90.06	87.34	90.68	86.93	88.26
Regional value of microbial metabolites	89.53	90.05	90.03	87.65	87.91
Regional value of fulvic acid substances	77.88	78.68	75.37	73.49	71.01
Regional value of humic acid substances	77.61	79.18	72.55	69.73	66.11

As seen in Table 3, there was a slight fluctuation in the similarity of the region values of aromatic protein substances during water treatment, starting from 90.06 % at the water inlet and finally reaching 88.26 % at the outlet. For the regional values of microbial metabolites, the similarity slightly increased from 89.53 % at the water inlet to 90.05 % at the anaerobic tank, and then slightly decreased during subsequent treatment, reaching 87.91 % at the outlet. The similarity of the regional values of humic acid substances started from 77.88 % at the water inlet and continued to decrease during the treatment process, reaching 71.01 % at the outlet. The similarity of the regional values of humic acid substances also showed a decreasing trend, from 77.61 % to 66.11 %. It can be seen that different types of organic substances exhibit distinct migration and transformation characteristics in the process of water treatment.

5. CONCLUSION

Under the current analytical technology growth, 3DEEM has been widely used in wastewater treatment monitoring due to its high sensitivity and strong resolution. With the acceleration of industrialization and the continuous increase of urban population, the concentration and types of organic pollutants in sewage are on the rise, bringing serious environmental pressure to water bodies. The study adopted a regional PCA based on 3DEEM to monitor the urban sewage treatment process, in order to accurately evaluate the treatment effect. The experimental results indicated that the trend of COD change can be quantified, decreasing from the initial 234 mg/L to 79 mg/L, reflecting significant degradation of organic pollutants after treatment, and thus improving treatment efficiency. The decrease in SI from 2.18×10^4 to 0.49×10^4 further confirmed the stability and reliability of the water treatment system in removing organic pollutants. In the PCA of water quality, the proportion of the first principal component increased from 86.51 % to 96.13 %, indicating the concentrated purification effect of the main pollutants and the enhanced stability in the effluent. The second principal component changed from 3.75 % to 3.99 %. The significant decrease of the third principal component in the aerobic pool, compared to 2.36–2.43 % in other stages, revealed the effectiveness of aerobic treatment in removing specific pollutants. The fourth principal component decreased from 2.18 % to 1.62 %, indicating a gradual degradation or transformation of its related indicators. It can be seen that the depth and accuracy of urban sewage treatment monitoring have been significantly improved, but there are still limitations. It is necessary to enhance the monitoring capabilities for pollutants that are difficult to degrade or detect, to further improve the efficiency and sustainability of urban sewage treatment.

ACKNOWLEDGEMENT

The research is supported by: The Major Science and Technology Projects of Henan Province (No.221100320200); Technological Research Project of Science and technology Department of Henan Province (No.252102111030); the Youth Project of Nanyang Normal University (No.2025QN009); Science and Technology Research Project of Nanyang (No.24KJGG014).

REFERENCES

[1] Brereton R. G. Numerical introduction to principal components analysis. *Journal of Chemometrics* 2022:36(8):2–6. https://doi.org/10.1002/cem.3405

[2] Brereton R. G. Introduction to residuals and estimation by principal components analysis. *Journal of Chemometrics* 2022:36(10):2–7. https://doi.org/10.1002/cem.3407

[3] Ito A., Yanase E. Study into the chemical changes of tea leaf polyphenols during Japanese black tea processing. *Food Research International* 2022:160(10):2–9. https://doi.org/10.1016/j.foodres.2022.111731

[4] Gao S., Zhang H., Li H., Pei Y. Synthesis of sulfur-chlorine-doped fluorescent carbon quantum dots from leachate membrane concentrate as a selective probe for Pd^{2+} detection. *Optical Materials* 2023:139(5):2–10. https://doi.org/10.1016/j.optmat.2023.113746

[5] Shi J., Jiang G., Sun Z., Guo F., Wang Q., Liu F. Dissolved organic matter tracers reveal contrasting characteristics in the concentrated flow zone and matrix-with-fractures zone of a sulfate-contaminated karst aquifer in South China. *Applied Geochemistry* 2022:146(1):105–431. https://doi.org/10.1016/j.apgeochem.2022.105431

[6] Venturini F., Sperti M., Michelucci U., Gucciardi A., Martos V. M., Deriu M. A. Extraction of physicochemical properties from the fluorescence spectrum with 1D convolutional neural networks: Application to olive oil. *Journal of Food Engineering* 2023:336(1):2–8. https://doi.org/10.1016/j.jfoodeng.2022.111198

[7] Lee S. N., Ahn J., Joo T. Coherent Vibrational Spectrum via Time-Resolved Fluorescence for Molecular Dynamics and Identification of Emitting Species-Application to Excited-State Intramolecular Proton Transfer. *The Journal of Physical Chemistry* 2022:126(30):4962–4968. https://doi.org/10.1021/acs.jpca.2c03263

[8] Xu R. Z., Cao J. S., Feng G. Fast identification of fluorescent components in three-dimensional excitation-emission matrix fluorescence spectra via deep learning. *Chemical Engineering Journal* 2022:43(P2):132893. https://doi.org/10.1016/j.cej.2021.132893

[9] Tang J., Chen C., Shen X., Xiao F., Li X. A three-dimensional positivity-preserving and conservative multimoment finite-volume transport model on a cubed-sphere grid. *Quarterly Journal of the Royal Meteorological Society* 2022:148(749):3622–3638. https://doi.org/10.1002/qj.4377

[10] Cheng P., Tian H., Xiao X., Gai H., Zhou Q., Zhou L. Influence of Thermal Maturity on the Time-Resolved Emission Spectrum (TRES) Fluorescence Lifetime Characteristics of Crude Oils: A Preliminary Study Based on a Thermal Simulation Experiment of Crude Oils. *Energy & Fuels* 2023:37(7):5165–5178. https://doi.org/10.1021/acs.energyfuels.3c00474

[11] Han L., Chen Y., Zhang H., Li G., Jia Q., Zhang S. Low-temperature synthesis of six-principal-component high-entropy transition-metal carbide aerogel thermal insulator. *Journal of the American Ceramic Society* 2023:106(2):841–847. https://doi.org/10.1111/jace.18856

[12] Xue H., Cui P., Tan J., Zhang G., Ge S., Cai X. Separation of principal component dihydromyricetin from Ampelopsis grossedentata by high-speed counter-current chromatography and its interaction with corn starch. *Journal of Food Science* 2022:87(6):2350–2363. https://doi.org/10.1111/1750-3841.16128

[13] Kassinopoulos M., Mitsis G. D. A multi-measure approach for assessing the performance of fMRI preprocessing strategies in resting-state functional connectivity. *Magnetic Resonance Imaging* 2022:85(1):228–250. https://doi.org/10.1016/j.mri.2021.10.028

[14] Ameek S., Josh B., Els P., Jan C. A Principal Component Analysis of polycyclic aromatic hydrocarbon emission in NGC 7023. *Monthly Notices of the Royal Astronomical Society* 2022:511(2):2186–2200. https://doi.org/10.1093/mnras/stac157

[15] Moreno Y. S., Bournival G., Ata S. Classification of flotation frothers – A statistical approach. *Chemical Engineering Science* 2022:248(PB):2–12. https://doi.org/10.1016/j.ces.2021.117252

[16] Zhang T., Yang Y., Zhang M., Jiang H., Yan Z., Liu J., Liu X. Effect of soy lecithin concentration on physiochemical properties and rehydration behavior of egg white protein powder: Role of dry and wet mixing. *Journal of Food Engineering* 2022:328(9):2–10. https://doi.org/10.1016/j.jfoodeng.2022.111062

[17] Hou Z., Tian H., Wang J. S., Zhang X., Song Q., Zheng R., Chen H., Chen B., Bai X., Chen Y. Three-dimensional Propagation of the Global Extreme-ultraviolet Wave Associated with a Solar Eruption on 2021 October 28. *The Astrophysical Journal* 2022:928(2):97–98. https://doi.org/10.3847/1538-4357/ac590d

[18] Tang W., Zhang L., Chen Q., Han M., Chen C., Liu W. Determination of monophenolase activity based on backpropagation neural network analysis of three-dimensional fluorescence spectroscopy. *Journal of Biotechnology* 2023:365(1):11–19. https://doi.org/10.1016/j.jbiotec.2023.02.001

[19] Brereton R. G. Introduction to statistical, algorithmic and theoretical basis of principal components analysis. *Journal of Chemometrics* 2022:36(9):2–9. https://doi.org/10.1002/cem.3406

[20] Shang L., Qiu A., Xu P., Yu F. Canonical Variate Nonlinear Principal Component Analysis for Monitoring Nonlinear Dynamic Processes. *Journal of Chemical Engineering of Japan* 2022:55(1):29–37. https://doi.org/10.1252/jcej.19we080

[21] Nsugbe E. Toward a Self-Supervised Architecture for Semen Quality Prediction Using Environmental and Lifestyle Factors. *Artificial Intelligence and Applications* 2023:1(1):35–42. https://doi.org/10.47852/bonviewAIA2202303